HHS Public Access

Author manuscript

Biomaterials. Author manuscript; available in PMC 2018 August 01.

Published in final edited form as:

Biomaterials. 2017 August ; 137: 1–10. doi:10.1016/j.biomaterials.2017.05.010.

Aortic Adventitial Fibroblast Sensitivity to Mitogen Activated Protein Kinase Inhibitors Depends on Substrate Stiffness

Rebecca A. Scott[1,2,4], **Prathamesh M. Kharkar**[2], **Kristi L. Kiick**[2,3,4], and **Robert E. Akins**[1,2,3,*]

[1]Nemours - Alfred I. duPont Hospital for Children, Wilmington, DE 19803

[2]Department of Materials Science & Engineering, University of Delaware, Newark, DE 19716

[3]Department of Biomedical Engineering, University of Delaware, Newark, DE 19716

[4]Delaware Biotechnology Institute, Newark, DE 19711

Abstract

Adventitial fibroblasts (AFs) are key determinants of arterial function and critical mediators of arterial disease progression. The effects of altered stiffness, particularly those observed across individuals during normal vascular function, and the mechanisms by which AFs respond to altered stiffness, are not well understood. To study the effects of matrix stiffness on AF phenotype, cytokine production, and the regulatory pathways utilized to interpret basic cell-matrix interactions, human aortic AFs were grown in 5%, 7.5%, and 10% (w/v%) PEG-based hydrogels with Young's moduli of 1.2, 3.3, and 9.6 kPa, respectively. In 5% gels, AFs had higher proliferation rates, elevated monocyte chemoattractant protein-1 secretion, and enhanced monocyte recruitment. Significantly more AFs were α-smooth muscle actin positive in 7.5% gels, indicating myofibroblast development. AFs in 10% gels had low proliferation rates but produced high levels of interleukin-6 and vascular endothelial growth factor-A. Importantly, these modulus-dependent changes in AF phenotype were accompanied by alterations in the mitogen-activated protein kinase (MAPK) pathways contributing to the production of cytokines. These data indicate that complex cell regulatory changes occur with altered tissue stiffness and suggest that therapeutics affecting MAPK pathways may have altered effects on AFs depending on substrate stiffness.

Keywords

hydrogel; fibroblast; mitogen-activated protein kinase; cytokine; vascular graft

*To whom correspondence should be addressed: Robert Akins, PhD, Director, Center for Pediatric Clinical Research and Development, Nemours - Alfred I. duPont Hospital for Children, 1600 Rockland Road, Wilmington, DE 19803, Ph: (302) 651-6811, Fax: (302) 651-6897, robert.akins@nemours.org.

1. Introduction

Although there have been significant advances in treatment, arterial diseases remain major causes of morbidity and mortality worldwide. Recently, the vascular adventitia has been identified as a critical mediator of arterial disease progression, with adventitial fibroblasts (AFs) implicated in the maladaptive cascades occurring in primary arterial disease and in vessel remodeling and restenosis after vascular intervention [1]. AFs can be activated to differentiate into migratory myofibroblasts [2], to secrete a number of cytokines, chemokines, growth factors, and proteases that affect vascular pathobiology and the behaviors of other resident adventitial cells [3], or to become quiescent and produce inflammatory mediators associated with the accumulation of activated vascular macrophage in diseased vessels [4, 5]. The actions of activated AFs further relate to the progressive extracellular matrix (ECM) remodeling [6, 7] and tissue stiffening [8, 9] that are hallmarks of vascular disease. In turn, matrix stiffness also influences AF phenotype [10]; thus, AFs are able to both alter substrate stiffness and respond to it in the context of adventitial function and disease progression.

Unfortunately, the interrelationships between AF phenotype, bioactive molecule expression, and the local biomechanical environment are not well understood, and it remains unclear how alterations in local tissue stiffness affect AF cell behavior, especially the secretion of key mediators. For example, production of interleukin-6 (IL-6) and monocyte chemoattractant protein-1 (MCP-1) by AFs results in the recruitment and activation of circulating and resident inflammatory cells to injured vascular tissue [11], while AF expression of vascular endothelial growth factor-A (VEGF) mediates endothelial cell growth and formation of neo-vasa vasorum [12]. Importantly, enhanced MCP-1, IL-6, and VEGF expression has been correlated with adventitial thickening, atherosclerosis, restenosis, and pulmonary hypertension [11, 13, 14], disease states in which matrix mechanics become strikingly altered compared to that of normal, healthy tissue [15].

In the context of vascular disease, mitogen-activated protein kinase (MAPK) pathways are important in cell proliferation, migration, and the regulation of inflammation, angiogenesis, and vascular tissue remodeling [16, 17]. Three well-characterized MAPK-family members are of particular interest: the extracellular signal-regulated kinase-1/2 (ERK-1/2), p38 MAPK, and Jun kinase (JNK) pathways can be activated by matrix mechanics to mediate cellular proliferation, differentiation, and stress responses [18, 19]. Although AFs are known to be mechanosensitive [20, 21], the contributions of MAPK activation to AF responses across different matrix moduli have not been thoroughly elucidated.

The complex structure of arterial walls allows for significant biomechanical strength, elasticity, and stiffness under certain conditions [22, 23]. At a cellular level, however, the average local stiffness of mammalian aortic artery adventitium has been measured at 15.8 kPa (with a range of 0.7 to 391kPa) [24]. Recent observations indicate that variations in matrix mechanics can regulate fibroblast morphology, proliferation, signaling pathways, and activation, leading to shifts in vascular remodeling [25, 26]. For example, AFs in injured arteries can convert to myofibroblasts [27] and alter the function and structure of the vessel wall by increasing the expression of ECM proteins or proteases, such as matrix

metalloproteinases (MMPs) [28]. Similar phenomena have been observed *in vitro* where several recent studies have confirmed that matrix stiffness significantly impacts the activation of fibroblasts, both initially and over time [10, 29, 30]. Our group has previously utilized poly(ethylene glycol) (PEG)-based hydrogels to evaluate the effects of substrate stiffness on vascular AFs in a 2D culture model [10]. This work, in addition to other studies [31, 32], corroborates that substrate stiffness, particularly at the lower end of the stiffness range for mammalian aortic artery adventitia, is a potent modulator of vascular cell activities, including proliferation, gene expression profiles, and differentiation status. Moving forward, *in vitro* cell culture systems could be of great use in determining the intracellular signaling mechanisms involved in AF responses to tissue stiffness, in providing insight into the mechanisms of arterial disease, and in identifying potential therapeutic approaches for regulating maladaptive vascular remodeling.

In this study, we utilized PEG hydrogel platforms to investigate the impact of matrix modulus on human AF activation in a 3D culture model. As small changes in stiffness are observed across individuals during normal vascular function, we were interested in using our hydrogel system to investigate how cells respond to small changes in stiffness, like those occurring prior to the initiation of complex pathophysiology and vascular disease. Here, AFs were encapsulated in hydrogels exhibiting physiologically-relevant moduli. Cell phenotype was examined by immunostaining for α-smooth muscle actin (αSMA), measuring THP-1 monocyte recruitment, and monitoring the production of inflammatory, angiogenic, and tissue remodeling factors. As previous work indicated that AFs were able to switch their phenotype relative to modulus, [10] we assessed the role of MAPK subfamilies in mediating stiffness-dependent changes in cell phenotype. This work serves to better understand the robust intracellular signaling mechanisms involved in cell response to microenvironmental cues, serving as an approach to advance current therapies and inform the development of new small-molecule and/or hydrogel-based treatments.

Methods

2.1 Peptide Synthesis & Characterization

To create PEG-based hydrogel platforms that allow AF-mediated remodeling and interaction with the hydrogel network, the matrix metalloproteinase (MMP)-sensitive peptide GGPQG↓IRGQGK (arrow indicates cleavage site) and the integrin binding peptide GRGDSPGK were utilized within hydrogel formations. Peptides were synthesized via solid-phase synthesis (Focus Xi, AAPPTec, Louisville, KY) with standard Fmoc chemistry. To create the bis-maleimide, end-functionalized, cell-degradable crosslinker peptide (mal-GGPQGIRGQGK-mal; MMP-MAL_2) and the monomaleimide-functionalized RGD peptide (GRGDSPGK-mal; RGD-Mal), maleimide functionalities were conjugated onto primary amine groups via 3-maleimidopropionic acid in DMF with HATU and DIEA. Maleimide functionalized peptides were cleaved from the resin in a TFA cleavage cocktail (95% TFA, 2.5% TIPS, and 2.5% H_2O), precipitated in cold diethyl ether, and dried in vacuo, prior to purification by reverse-phase high-performance liquid chromatography (Waters, Millford, MA). The molecular weight of the desired product was confirmed by electrospray ionization mass spectroscopy (ESI-MS) using a Thermo Finnegan LCQ Advantage mass spectrometer

(MMP-Mal_2: 1400 kDa; RGD-Mal: 1000 kDa) and the average number of maleimide groups per MMP-MAL_2 peptide was determined to be ~1.8, via ^{1}H NMR using an AVIII 600 MHz NMR spectrometer (Bruker, Billerica, MA). Peptide purity was 95% and 92% for MMP-MAL_2 and RGD-Mal peptides, respectively. Peptides were stored as lyophilized powder at −20°C until use.

2.2 Hydrogel Formation

Hydrogels were formed by crosslinking of four-arm thiol-functionalized poly(ethylene glycol) (PEG-SH_4; f=4, Mn 10,000 g/mol, JenKem Technology, Allen, TX), with the MMP-Mal_2 and RGD-Mal peptides. Hydrogels were prepared at concentrations of 5%, 7.5%, and 10% (w/v%) by altering the concentrations of PEG-SH_4 and MMP-Mal_2, while the concentration of RGD-Mal was held constant at 1 mmol/L, independent of w/v%. Hydrogels were crosslinked at a thiol to maleimide residue ratio of 1:1 for all formulations. As such, hydrogels of a concentration of 5% comprised 3.9 mmol/L PEG-SH_4 and 7.2 mmol/L MMP-Mal_2; 7.5% hydrogels comprised 5.8 mmol/L PEG-SH_4 and 11.1 mmol/L MMP-Mal_2; and 10% hydrogels comprised 7.8 mmol/L PEG-SH_4 and 15.0 mmol/L MMP-Mal_2. To form hydrogels, PEG-SH_4, MMP-Mal_2, and RGD-Mal were independently dissolved in buffer (10 mmol/L sodium phosphate monobasic monohydrate, 5 mmol/L citric acid trisodium salt anhydrous, 140 mmol/L sodium chloride, pH 4.8) and sterilized through a 0.2 μm PVDF filter. Maleimide- and thiol-containing solutions, along with 10 mmol/L HEPES in HBSS (1/5 of the final gel volume; pH 7.4), were mixed together via simple pipetting and deposited onto cell culture dishes. Hydrogels were allowed to crosslink for 15 mins at 37°C, prior to being immersed in cell culture medium.

2.3 Adventitial Fibroblast Culture and Encapsulation in Hydrogels

Human aortic AFs (unidentified 53 yo male donor; Lonza, Allendale, NJ) were cultured in stromal cell growth medium (SCGM), which comprised stromal cell basal medium supplemented with 5% FBS, basic fibroblast growth factor, and insulin (all from Lonza). Cells were maintained at 37°C with 5% CO_2 and used between passage numbers 4 and 7 for all assays. AF phenotype was characterized by examining cell morphology and proliferative capacity and by verifying that fewer than 10% of the cells were positive for α-smooth muscle actin, a marker of myofibroblasts, at each passage.

To encapsulate cells in hydrogels, AFs were suspended in 10 mmol/L HEPES in HBSS and added to the hydrogel precursor solutions to achieve 2×10^5 cells/mL gel, unless otherwise noted. As understanding the impact of cell-matrix interactions was the primary focus of this work, we utilized this low seeding density in order to reduce the potential for confounding cell-cell interactions. Once mixed, 50 μL volumes of hydrogel were placed on glass bottom dishes (MatTek Corporation, Ashland, MA), allowed to gel for 15 mins at 37°C, and immersed in 2 mL of SCGM, unless otherwise noted. For MAPK inhibitor studies, freshly-prepared hydrogels were immersed in SCGM supplemented with 10 μmol/L of the ERK-1/2 pathway inhibitor PD98059, the p38 inhibitor SB203580, or the JNK inhibitor SP600125 (all from Enzo Life Sciences). Medium was not replaced over the duration of these experiments. Medium was collected on days 1, 3, and 7, and stored at −80°C for further analysis.

2.4 Rheological Characterization of Hydrogels

The mechanical properties of the hydrogels were characterized via bulk oscillatory rheology (AR-G2, TA instruments). Briefly, the hydrogel precursor solutions were added to a cylindrical mold (30 mL; diameter = 4.6 mm, thickness = 1.8 mm) and allowed to gel for 15 mins at 37°C. In some rheology experiments, AFs were encapsulated in the hydrogels as described above. Hydrogels were subsequently immersed in 2 mL of SCGM and incubated at 37°C with 5% CO_2. The elastic storage moduli of the hydrogels were measured at 24 hrs and 7 days using a 20-mm diameter stainless steel, parallel plate geometry. Time sweep measurements were obtained within the linear viscoelastic regime using 2% constant strain and 2 rad/s angular frequency. A normal force of 0.2 N was applied to prevent slipping during measurement. The shear modulus (G') was measured and converted to Young's modulus (elastic modulus, E) using the formula $E = 2G'(1 + \nu)$ with $\nu = 0.5$ [33].

2.5 Cell Proliferation and Viability

At indicated time points, the hydrogel cultures were washed with PBS, flash frozen in liquid nitrogen, and stored at −20°C until use. A Quant-iT™ Picogreen® dsDNA assay (Life Technologies) was used to measure total DNA content of the harvested samples. Briefly, after thawing, the samples were digested overnight at 65°C with 180 μg/mL papain (Sigma) diluted in PBS containing 4 mmol/L ethylenediaminetetraacetic acid (Sigma) and 10 mmol/L L-cysteine hydrochloride (Sigma). Samples were cooled to room temperature and centrifuged at 0.1×g for 1 min to remove debris, before collecting the supernatant for analysis via Picogreen dsDNA assay, prepared as instructed by the manufacturer. Samples and DNA standards were measured in this assay in triplicate. The number of AFs within each gel at each time point was determined from the total amount of DNA in each sample. Average proliferation rate was then defined as difference in the number of cells over the time course normalized to duration of the time course. For the 3D culture samples, the fluorescence signals obtained from blank hydrogels (i.e. without cells, cultured and processed similarly to those with cells) were used as background values.

To assess the viability of AFs in hydrogels, a live/dead assay was performed at specified time points. Briefly, 2 μmol/L calcein-AM (Life Technologies) and 4 μmol/L ethidium homodimer-1 (Life Technologies) in PBS were added to gels; gels were incubated at 37°C for 20 mins and washed 3 times in PBS. Cells were visualized using a Zeiss 510 confocal microscope with a 10x Plan-Neofluar 0.3 N.A. objective. Three scan volumes were completed in distinct locations for each culture with an xy area of 512 μm^2 and a z depth of 100 μm (4.26 μm per step).

2.6 Immunostaining for a-smooth muscle actin and F-Actin

To distinguish cells progressing towards a myofibroblastic lineage, cultures were fixed in 4% paraformaldehyde for 30 min, permeabilized with 0.1% Triton X-100 (Sigma) in PBS for 1 hr, and blocked in 3% bovine serum albumin (Sigma) in PBS for 1 hr. α-smooth muscle actin (αSMA), a marker of myofibroblast differentiation, was labeled using mouse anti-human αSMA (1:100; Abcam, Cambridge, MA) overnight at 4°C. Sam ples were washed and incubated with the secondary antibody, goat anti-mouse AlexaFluor® 555 (1:500; Life Technologies), phalloidin-488 (1:100; Life Technologies), and the nuclear stain Hoescht

33258 (1:5000; Life Technologies) overnight at 4°C. Cells were visualized using an Olympus BX-60 fluorescence microscope equipped with an Evolution QEi monochrome 12-bit digital camera (Media Cybernetics) controlled by Image Pro Plus software (version 7.0; Media Cybernetics). Using a 20× objective, three scan volumes were completed in distinct locations for each gel with an xy area of 550 μm × 410 μm, with a z depth of 200 μm (1 μm per step). Transitional AF percentages were quantified by manually counting cells expressing αSMA.

2.8 Protein Quantification via ELISA

Human IL-6, MCP-1, and VEGF-A ELISA development kits (Peprotech, Rocky Hill, NJ) and MMP-2 and MMP-9 Quantikine ELISA kits (R&D Systems, Minneapolis, MN) were used according to the manufacturers' instructions. To account for variance in AF number in hydrogel cultures, the amount of protein detected in each sample of culture medium was normalized to the amount of DNA in the corresponding gel.

2.7 Migration of THP-1 Monocytes in Response to AF-gel-conditioned Medium

THP-1 cells (American Type Culture Collection, Manassas, VA; ATCC), a human leukemic promonocytic cell line, were cultured in RPMI 1640 medium (ATCC) containing 10% FBS (Life Technologies). To evaluate THP-1 transmigration in response to AF cytokine production, AFs were encapsulated at a density of 4×10^5 cells/mL gel and cultured in SCGM media. After 3 days of culture, AF conditioned media was collected. The migration of THP-1 cells towards AF-conditioned medium was assessed using modified Boyden chambers with polycarbonate membrane inserts with 5-μm pores (Sigma). Briefly, THP-1 cells were labeled with 2 μmol/L calcein-AM, resuspended in serum-free SCGM at a concentration of 2×10^6 cells/mL, and 100 μL of cells were placed above the Transwell inserts. Conditioned medium or control SCGM (600 μL/well) was placed below the inserts, and plates were incubated at 37°C for 2 hrs to allow for THP-1 cell migration. Transwell inserts were removed and a fluorescent measurement of the calcein-labeled THP-1 cells that migrated into the control medium or conditioned SCGM was analyzed in triplicate using a PerkinElmer VICTOR X4 2030 Multilabel Plate Reader (PerkinElmer, Waltham, MA) at excitation/emission wavelengths of 485 nm/535 nm. The number of THP-1 cells that migrated was then determined by comparing to a standard curve of known numbers of calcein-labeled THP-1 cells. To account for the specific number of AFs contributing to migration in each case, THP-1 migration data were further normalized to the number of AFs in the corresponding gel.

2.9 Statistics

Data are expressed as the mean ± standard error of the mean, unless otherwise noted. Statistical comparisons between hydrogel modulus and proliferation were performed by one-way analysis of variance (ANOVA) using Tukey HSD post-hoc tests. A two-way ANOVA was used to analyze differences in αSMA-positive cells, viability, and protein expression between group, day, and group by day interaction. If the F-test revealed significant statistical differences at the 0.05 level, pairwise comparisons were made using Tukey HSD post-hoc. A p-value of <0.05 was considered significant. Statistical interpretations were made using SPSS version 23 (SPSS, IBM).

3. Results

3.1 Formation of hydrogels with varying matrix moduli

To form degradable PEG-based hydrogels, thiol end-functionalized PEG macromers (PEG-SH_4) and maleimide end-functionalized peptides (Fig. 1) were used to generate stable crosslinks via a Michael-type addition reaction [34, 35], a class of highly efficient click reactions that occur under physiological conditions without deleterious byproducts. PEG-SH_4 was combined at room temperature with a bis-maleimide, end-functionalized, MMP-sensitive crosslinker peptide (MMP-Mal_2) to form highly elastic, degradable hydrogels that accommodate cell-mediated remodeling of the matrix via protease degradation. As collagen is the predominant structural protein found in the adventitia, AF interactions with the hydrogel network were facilitated through the incorporation of mono-maleimide pendent RGD peptides (RGD-Mal). Pilot assessments showed no differences in AF proliferation across gels containing 0.3–3 mM RGD (data not shown); thus, we examined the behavior of AFs in hydrogels containing 1 mM RGD-Mal in this study. Polymer concentration was varied to permit assessment of the response of encapsulated AFs to materials with various moduli.

Gelation kinetics were measured via oscillatory shear rheology, a technique in which a test specimen is subjected to oscillatory stress, using dynamic time sweep assays in the linear viscoelastic regime. Representative storage moduli (G') and loss moduli (G"), which represent the elastic and viscous component of the hydrogel, respectively, were evaluated during gel formation (Fig. S1). These materials form highly elastic networks within ca. 110, 80, and 55s for the 5%, 7.5%, and 10% gels, respectively, as indicated by a crossover point between the storage and loss moduli, which is an indirect measurement of gel point. To relate the mechanical properties of our hydrogel formulations to the range of moduli reported for adventitial tissue (0.7 to 391 kPa) [24], the equilibrium storage modulus of AF-laden hydrogels was measured and converted to Young's modulus [33]. The equilibrium Young's moduli for 5%, 7.5%, and 10% hydrogels containing AFs, measured after 24 hrs of incubation at 37°C in SCGM medium, were 1.2, 3.3, and 9.6 kPa, respectively (Fig. 2A). To determine whether encapsulated AFs actively remodeled these matrices, we assessed gel moduli after 7 days of culture. AF-laden hydrogels remained mechanical stable after 7 days of culture. However, AF-mediated hydrogel remodeling resulted in a 36% ± 6% and 35% ± 5% reduction in the bulk modulus of 5% and 7.5% hydrogels, respectively, while 10% gels exhibited a reduction in bulk modulus of 25% ± 2%, after 7 days of culture (Fig. 2B). The decrease in hydrogel mechanical properties confirms that encapsulated AFs are able to remodel the surrounding hydrogel, presumably via cleavage of the MMP-sensitive peptide incorporated in the hydrogels.

3.2 Matrix modulus impacts AF proliferation rate

As ECM elasticity can regulate cell proliferation, we examined the impact of hydrogel modulus on the proliferation of encapsulated AFs. Proliferation was highest in 5% gels and decreased with increasing gel modulus (Fig. 3A). AFs in 5% hydrogels exhibited an average proliferation rate of 1150 ± 140 new cells/day. AFs in 7.5% and 10% hydrogels had significantly lower proliferation rates in comparison, where 380 ± 140 and 110 ± 50 new

cells/day were observed, respectively. Importantly, AFs encapsulated in 5%, 7.5%, and 10% gels were homogenously distributed throughout the gel and maintained high viability (>90%) over the entire 7-day experiment (Fig. 3B, Fig. S2).

3.3 Low modulus hydrogels stimulate diffuse α-smooth muscle actin in AFs

To determine the impact of matrix modulus on AF phenotype and the appearance of myofibroblasts, encapsulated AFs were immunostained for αSMA (Fig. 4A). Diffuse αSMA staining was observed in a sub-population of AFs in all hydrogels after 1 day of culture, where 8.6%-19.0% of cells were positive for αSMA (Fig. 4B). The percentage of αSMA-positive cells significantly increased in both 5% and 7.5% hydrogels after 7 days. The percentage of αSMA-positive AFs was most prominent in 7.5% hydrogels, where 74.3% ± 5.1% of cells displayed diffuse αSMA. Conversely, 2.2% ± 2.1% of AFs in 10% hydrogels were αSMA-positive after 7 days.

3.4 Hydrogel modulus alters AF secretion of chemotactic, angiogenic, and matrix remodeling factors

As THP-1 monocyte recruitment by encapsulated AFs was observed to be modulus-dependent, we evaluated MCP-1 and IL-6 production by AFs within hydrogels. MCP-1 secretion by AFs was dependent on hydrogel modulus (Fig. 5A). After 3 days of culture, MCP-1 production was highest in 5% hydrogels, where cells secreted 29.0 ± 0.4 pg MCP-1/ng DNA; AFs in 7.5% and 10% gels secreted significantly less MCP-1 (18.2–20.3 pg MCP-1/ng DNA). Increased MCP-1 production was observed in all hydrogel formulations when conditioned medium was sampled on day 7; however, MCP-1 levels remained highest in 5% hydrogels. Conversely, significant differences in IL-6 protein levels were not observed across hydrogel groups after 3 days of culture, where cells in all gels produced 44.8–55.7 pg IL-6/ng DNA (Fig. 5B). IL-6 production by AFs in 5% hydrogels remained similar at 7 days, as only 50.8 ± 4.3 pg IL-6/ng DNA was detected. Significant increases in IL-6 were observed in 7.5% and 10% hydrogels, where AFs produced 73.1 ± 14.0 and 74.4 ± 7.6 pg IL-6/ng DNA, respectively.

Production of inflammatory chemokines following vascular injury is typically accompanied by angiogenesis [36], thus we examined VEGF production by AFs. VEGF secretion by AFs was dependent on hydrogel modulus (Fig. 5C), with secretion increasing with increasing modulus. After 3 days of culture, AFs in the 5% hydrogels produced 0.65 ± 0.1 pg VEGF/ng DNA, while significantly higher VEGF secretion (1.3–1.6 pg VEGF/ng DNA) was detected in the 7.5% and 10% hydrogels. VEGF production significantly increased in all hydrogels with time; however, VEGF levels remained highest in stiffer modulus hydrogels, where VEGF levels peaked at 4.9 ± 0.4 pg VEGF/ng DNA in the 10% hydrogels after 7 days.

Finally, MMP-2 and MMP-9, which are produced by AFs during arteriogenesis and disease progression and have been shown to play a role in AF phenotype transition and in tissue remodeling in the progression of vascular disease [28, 37], secretion was examined. After 3 days of culture, MMP-2 production by AFs was initially independent of hydrogel modulus, where 128.7–157.5 pg MMP-2/ng DNA was detected for all hydrogel formulations after 3 days of culture (Fig. 5D). However, after 7 days of culture, AFs encapsulated in 7.5%

hydrogels produced significantly more MMP-2 (681.6 ± 64.0 pg MMP-2/ng DNA) compared to cells in either 5% or 10% gels (401.4–466.0 pg MMP-2/ng DNA). Interestingly, MMP-9 production was not detected in any of the experiments conducted. Regardless, our results here indicate that AF production of signaling molecules related to chemotaxis, angiogenesis, and remodeling is significantly influenced by matrix stiffness.

3.5 Encapsulated AFs recruit monocytes in a modulus-dependent manner

The release of factors that recruit monocytes is a key function of AFs in vessel remodeling [5]. To investigate the impact of hydrogel modulus on AF recruitment of monocytes, we performed THP-1 transmigration assays using Boyden chambers with conditioned medium, obtained from AFs encapsulated in 5%, 7.5%, and 10% hydrogels and cultured for 3 days, as the attractant. THP-1 transmigration was significantly increased in response to conditioned medium obtained from AF-laden hydrogels after 2 hrs of exposure, compared to transmigration towards medium obtained from a cellular hydrogel controls or fresh SCGM (Fig. 6A). Maximally, a 3.8-fold increase in transmigration was observed in response to conditioned medium from 5% gels containing AFs when compared to migration in response to fresh SCGM. Interestingly, the number of migratory THP-1 cells was lower in response to conditioned medium obtained from higher modulus hydrogels.

To distinguish whether enhanced monocyte migration in low stiffness gels stemmed simply from an elevated AF number resulting in increased total cytokine secretion rather than reduced cytokine production per cell, we normalized the number of transmigrated THP-1 to the number of AFs in the corresponding hydrogel (Fig. 6B). Following normalization, no significant differences were observed between hydrogels indicating that enhanced monocyte migration in low stiffness gels stemmed from enhanced AF numbers leading to increased total cytokine secretion, and not from reduced cytokine production per cell.

3.6 AF proliferation is regulated by ERK-1/2 and JNK in low modulus gels

MAPK activation has been linked to matrix mechanics and to vascular cell proliferation. Accordingly, we investigated the role of MAPK subfamilies, including the ERK-1/2, p38, and JNK pathways, by inhibiting their activity in AFs and monitoring the subsequent response. To simplify our study of MAPK antagonism and improve the statistical design and power of our approach, we focused our investigation to AFs encapsulated in 5% and 10% hydrogels. The addition of MAPK inhibitors to cultures did not alter AF viability (Fig. S3); however, AF proliferation was altered in certain instances following treatment with specific inhibitors. For example, a decrease in proliferation rate was observed when AFs in 5% hydrogels were treated with either the JNK inhibitor SP600125 or the ERK-1/2 pathway inhibitor PD98059, compared to control cells treated with DMSO (Fig. 7A). Interestingly, AF proliferation rate was not altered in 5% gels treated with the p38 inhibitor SB203580. The addition of the MAPK inhibitors to 10% hydrogels did not alter AF proliferation rate, compared to DMSO controls (Fig. 7B).

3.7 MAPKs regulate AF production of IL-6, MCP-1, VEGF, and MMP-2

As the MAPK subfamilies critically regulate the expression of inflammatory, angiogenic, and tissue remodeling molecules, we sought to determine their role in the differential

production patterns of MCP-1, IL-6, VEGF, and MMP-2 by AFs encapsulated in our hydrogel system. The effect of MAPK inhibitors on these factors was examined at both 3 and 7 days of culture, with similar trends apparent at both time points. Here, we describe the effect of MAPK pathway inhibitors on molecule expression after 3 days of culture (Fig. 8). Similar trends in expression were observed after 7 days of culture with MAPK pathway inhibitors, the results for which can be found in the supplemental information (Fig. S4).

The inhibition of the different MAPK pathways on AF factor production depended on hydrogel modulus. MCP-1 production by AFs in 5% hydrogels was significantly reduced following inhibition of ERK-1/2 pathways by PD98059 (22.0% reduction), p38 by SB203580 (82.8% reduction), or JNK by SP600125 (68.2% reduction) compared to DMSO controls (Fig. 8A). In the stiffer 10% hydrogels, a decrease in MCP-1 production was observed only after inhibition of JNK (47.4% reduction). Similar to MCP-1, IL-6 production by AFs in the 5% hydrogels was significantly reduced following treatment with the p38 inhibitor SB203580 (53.3% reduction) or the JNK inhibitor SP600125 (64.5% reduction), compared to DMSO controls (Fig. 8B). In contrast to our observations of MCP-1 production, ERK-1/2 pathway inhibition with PD98059 did not affect IL-6 levels. In the stiffer 10% hydrogels, JNK inhibition reduced IL-6 production (68.6% reduction) as it did MCP-1; however, blockade of p38 with SB203580 or ERK-1/2 pathways with PD98059 also resulted in reduced IL-6 secretion (46.4% and 43.3% reduction, respectively) by AFs; whereas, these inhibitors did not have a significant effect on MCP-1.

Each of the MAPK pathways investigated was highly involved in regulating VEGF production by AFs. Although AFs in 10% gels produced more VEGF, the inhibitor effects appeared to be independent of stiffness (Fig. 8C). VEGF production was significantly decreased following treatment with the ERK-1/2, p38, and JNK inhibitors in both 5% and 10% hydrogels. For both hydrogel moduli examined, VEGF secretion was reduced on average by 61.6%, 92.8%, and 67.0%, when cultures were treated for 3 days with PD98059, SB203580, or SP600125, respectively. In contrast, MMP-2 production was not regulated by all MAPK subfamilies (Fig. 8D). In softer 5% hydrogels, a significant reduction in MMP-2 secretion was observed only when AFs were treated with the p38 inhibitor SB203580. Interestingly, in 10% hydrogels, p38 inhibition did not appear to play a regulatory role in MMP-2 production. Rather, only JNK inhibition by PD600125 affected MMP-2 production (20.2% reduction) in stiffer gels.

4. Discussion

AFs are key regulators in the maladaptive cascades, progressive ECM remodeling, and tissue stiffening that arise in vascular disease [6–9]. However, elucidation of the detailed relationships that link cell phenotype, cytokine production, and the local biomechanical environment to vascular disease progression is difficult with current *in vivo* models. Hydrogel platforms provide dynamic and versatile *in vitro* models to gain insight into cell activation in response to matrix alterations [10, 29, 31, 32, 38], and can be used to probe fundamental mechanisms contributing to homeostasis and disease progression. Our studies on PEG hydrogels, displaying moduli relevant to the local stiffness of mammalian aortic artery adventitium (0.7–391 kPa), [24] demonstrate that AFs not only switch their phenotype

relative to modulus, but that they also alter the MAPK subfamilies used to interpret basic cell-matrix interactions, suggesting that therapeutics targeted towards MAPK pathways have altered effects on AFs with altered arterial stiffness. An understanding of how cell-matrix interactions are translated will allow for more precise application of current therapies and the development of new treatments.

While it remains unknown how cell-matrix interactions drive cell function, several groups have demonstrated the importance of MAPK pathways, which can be activated by mechanical stimuli, in the progression of vascular disease [16, 17, 39]. AFs are known to be mechanosensitive [20, 21]. For example, AFs exposed to mechanical stretch exhibited increased expression of collagen 1α1, 3α1, and 5α1 mRNA, which was correlated to enhanced p38 phosphorylation [40]. However, the contributions of MAPK activation to AF responses to different matrix moduli have not been thoroughly elucidated. Here, we utilized PEG-based hydrogel platforms to investigate the impact of alterations in local tissue stiffness on AF cell phenotype and any corresponding cell-matrix translation via MAPK pathways. Hydrogel concentrations of 5%, 7.5%, and 10% (w/v%) were selected to give a narrow range of physiologically relevant moduli, 1.2–9.6 kPa, for vascular cell studies as motivated by our and others' previous work with materials of this composition [10, 32]. Although the stiffness of our gels was toward the lower end of the stiffness range for mammalian aortic artery adventitia, this range is highly relevant for vascular cell studies and is consistent with the small changes in stiffness that are readily observed across individuals during normal vascular function.

Although the mechanisms by which AFs sense vascular injury and changes in their surrounding microenvironment have yet to be fully elucidated, increased MMP activity is thought to be necessary for AFs, in particular adventitial myofibroblasts, to migrate through the adventitial matrix following arterial injury [41]. Interestingly, AFs in 7.5% hydrogels produced 1.7-fold more MMP-2 after 7 days of culture, compared to cells in softer 5% and stiffer 10% gels; data which further corresponded to an increased number of αSMA-positive AFs in 7.5% hydrogels after 7 days. It should be noted that while differentiated f-actin stress fibers were observed, the staining patterns for αSMA were diffuse and likely representative of a transitional protomyofibroblast phenotype, rather than fully-differentiated myofibroblasts [42]. Nonetheless, the appearance of αSMA-positive cells was associated with the initial gel w/v% and the relationship between modulus and AF activation, and subsequent behavior, was non-linear. Although these results appear to be counterintuitive based on myofibroblast-like cells in other settings [31, 43], we have previously observed similar non-linear trends in gene expression as a function of hydrogel stiffness for genes related to AF phenotype and CD34+ stem cell maintenance [10, 32]. Similarly, non-linear patterns in fibroblast [44] and smooth muscle cell [45] motility, neurite extension [46], and transcription factors related to epithelial-to-mesenchymal transition in cancer cells [47] have been observed across a range of extracellular matrix rigidities. Clearly, cell behavior and phenotype in response to changes in stiffness can be regulated using non-linear mechanisms, and our results may pave the way for further investigation into this paradigm.

Activated AFs can transition toward a migratory myofibroblast phenotype; however, quiescent AFs can also produce signals to recruit and activate leukocytes [4, 5]. In our study,

AFs in 10% hydrogels were less proliferative and fewer were positive for αSMA than cells in softer gels. These observations suggest that AFs in higher modulus hydrogels were quiescent, and we sought to investigate whether they would recruit more THP-1 monocytes than cells in softer gels. In contrast to these expectations, THP-1 transmigration was highest when monocytes were exposed to conditioned medium obtained from AF-laden 5% hydrogels; data that correlated with increased MCP-1 protein expression in softer gels. As AFs appeared to neither be activated nor stimulated to produce chemokines in 10% gels, our results suggested that AFs in 10% gels exhibit phenotypes consistent with those found in healthy tissue. However, IL-6 production was increased in the higher modulus gels at longer time points. Interestingly, individuals with hypertension, a disease state associated with altered vascular tone, exhibit chronically increased tissue levels of IL-6 [48]. Thus, our results indicate that elevated modulus influences a chronic IL-6 response from AFs, which is uncoupled from other disease and AF activation phenomena in this system.

The specific signaling pathways utilized by encapsulated AFs provide insight into how alterations in matrix stiffness during vascular disease progression regulate AF phenotype. A primary route for matrix stiffness to affect cells is through the MAPK subfamilies, which are implicated in the progression of vascular disease [16–19]. In this study, we used an antagonistic strategy to elucidate the functions of intracellular signaling pathways ERK-1/2, p38, and JNK in regulating AF phenotype. To simplify our study of MAPK antagonism and improve the statistical design and power of our approach, we focused our investigation to AFs encapsulated in 5% and 10% hydrogels. Our assays did not discern variations in AF proliferation under the higher stiffness condition, likely due to the low proliferation rate observed in these 10% gels. However, our approach demonstrated that AF proliferation in the lower modulus gels and protein production in both 5% and 10% hydrogels were in part differentially regulated through the MAPK subfamilies. In some compelling instances, AFs utilized distinctly different pathways for the translation of matrix stiffness information (Table 1). For example, the ERK-1/2 pathway is involved in IL-6 production by AFs encapsulated in 10% hydrogels, but not from cells within 5% gels, perhaps explaining the enhanced IL-6 production observed in 10% hydrogels by otherwise quiescent AFs. Conversely, while AFs in 5% and 10% gels produced similar levels of MMP-2, MMP-2 elevation is sensitive to p38 inhibition in 5% hydrogels (but not 10%) and to JNK inhibition in 10% hydrogels (but not 5%). Thus, we demonstrate here that AFs not only switch their phenotype relative to modulus, but they also switch the pathways used to interpret basic cell-matrix interactions.

Interestingly, MAPK regulation of VEGF expression was not modulus dependent, as inhibition of ERK-1/2, p38, and JNK all resulted in decreased VEGF secretion in both 5% and 10% hydrogels. These observations suggest that while MAPK subfamilies do serve as important regulators of VEGF production, they are not involved in stiffness-mediated changes in MAPK pathway signaling. Further, VEGF expression was found to increase with increased hydrogel modulus; interestingly, while hypoxia is known to elevate VEGF production in human cardiac and adventitial fibroblasts [49, 50], the hydrogels in our studies exhibited similar swelling capacities, upwards of 97%, corresponding to similar pore sizes (13.1–15.2 nm), as calculated using the Flory-Rehner equation (Table S1). Thus, diffusional limitations were similar across gel formulations, and any differences in local pO_2 levels

were unlikely to be related to diffusion. Thus, VEGF production by encapsulated AFs here is likely attributed to cellular activities associated with altered hydrogel modulus; this interpretation is supported by previous reports demonstrating that increased VEGF levels correlate with decreased carotid distensibility (i.e., increased stiffness) [51].

In conclusion, we demonstrate that AF phenotype was critically dependent on substrate modulus, as shown by alterations in AF proliferation, myofibroblast transdifferentiation, and secretion patterns for signaling molecules in our *in vitro* hydrogel platforms. We further show that the MAPK subfamilies mediate stiffness-dependent changes in cell phenotype and AFs were found to switch the MAPK subfamilies used to interpret basic cell-matrix interactions in a stiffness dependent manner. These results emphasize the complicated and robust mechanisms associated with intracellular signaling pathways relevant to disease progression. Our data suggests that arterial stiffness may impact the efficacy of therapeutics targeting MAPK pathways on AFs. A limitation, however, is that due to human donor availability, we were only able to examine AFs isolated from a single donor in this work. Future work focusing on donor-specific responses, particularly investigating the impact of donor age and gender on AF activity, will be necessary. Additional studies resolving the relationships between signaling pathways, matrix stiffness, and cell behavior will be critical to our further understanding of vascular disease progression, particularly with respect to AF proliferation in the context of arterial disease, and the development of advanced therapies.

Supplementary Material

Refer to Web version on PubMed Central for supplementary material.

Acknowledgments

The authors would further like to thank Nile Bunce for technical help with peptide synthesis. This research was made possible by funds from the Nemours Foundation and by support from the NHLBI (R01 HL108110, F32 HL127983). Instrumentation resources were provided by support from the NIGMS (P30 GM110758, U54 GM104941, and S10 OD016361).

References

1. Goel SA, Guo L-W, Liu B, Kent KC. Mechanisms of post-intervention arterial remodelling. Cardiovasc Res. 2012; 96:363–71. [PubMed: 22918976]
2. Sartore S, Chiavegato A, Faggin E, Franch R, Puato M, Ausoni S, et al. Contribution of adventitial fibroblasts to neointima formation and vascular remodeling: from innocent bystander to active participant. Circulation research. 2001; 89:1111–21. [PubMed: 11739275]
3. Davie NJ, Gerasimovskaya EV, Hofmeister SE, Richman AP, Jones PL, Reeves JT, et al. Pulmonary artery adventitial fibroblasts cooperate with vasa vasorum endothelial cells to regulate vasa vasorum neovascularization: A process mediated by hypoxia and endothelin-1. Am J Pathol. 2006; 168:1793–807. [PubMed: 16723696]
4. Chen B-R, Cheng H-H, Lin W-C, Wang K-H, Liou J-Y, Chen P-F, et al. Quiescent fibroblasts are more active in mounting robust inflammatory responses than proliferative fibroblasts. PLoS ONE. 2012; 7:e49232. [PubMed: 23155470]
5. El Kasmi KC, Pugliese SC, Riddle SR, Poth JM, Anderson AL, Frid MG, et al. Adventitial fibroblasts induce a distinct pro-inflammatory/pro-fibrotic macrophage phenotype in pulmonary hypertension. J Immunol. 2014; 193:597–609. [PubMed: 24928992]
6. Galis ZS, Khatri JJ. Matrix metalloproteinases in vascular remodeling and atherogenesis: The good, the bad, and the ugly. Circulation research. 2002; 90:251–62. [PubMed: 11861412]

7. Stenmark KR, Davie N, Frid M, Gerasimovskaya E, Das M. Role of the adventitia in pulmonary vascular remodeling. Physiology. 2006; 21:134–45. [PubMed: 16565479]
8. van Popele NM, Grobbee DE, Bots ML, Asmar R, Topouchian J, Reneman RS, et al. Association between arterial stiffness and atherosclerosis: The rotterdam study. Stroke. 2001; 32:454–60. [PubMed: 11157182]
9. Cecelja M, Chowienczyk P. Role of arterial stiffness in cardiovascular disease. JRSM Cardiovasc Dis. 2012
10. Robinson KG, Nie T, Baldwin A, Yang E, Kiick KL, Akins RE. Differential effects of substrate modulus on human vascular endothelial, smooth muscle, and fibroblastic cells. J Biomed Mater Res A. 2012; 100:1356–67. [PubMed: 22374788]
11. Tieu BC, Lee C, Sun H, LeJeune W, Recinos A 3rd, Ju X, et al. An adventitial IL-6/MCP1 amplification loop accelerates macrophage-mediated vascular inflammation leading to aortic dissection in mice. J Clin Invest. 2009; 119:3637–51. [PubMed: 19920349]
12. Kuwahara F, Kai H, Tokuda K, Shibata R, Kusaba K, Tahara N, et al. Hypoxia-inducible factor-1α/vascular endothelial growth factor pathway for adventitial vasa vasorum formation in hypertensive rat aorta. Hypertension. 2002; 39:46–50. [PubMed: 11799077]
13. Savale L, Tu L, Rideau D, Izziki M, Maitre B, Adnot S, et al. Impact of interleukin-6 on hypoxia-induced pulmonary hypertension and lung inflammation in mice. Resp Res. 2009; 10:6.
14. Nykänen AI, Krebs R, Saaristo A, Turunen P, Alitalo K, Ylä-Herttuala S, et al. Angiopoietin-1 protects against the development of cardiac allograft arteriosclerosis. Circulation. 2003; 107:1308–14. [PubMed: 12628953]
15. Ponticos M, Smith BD. Extracellular matrix synthesis in vascular disease: hypertension, and atherosclerosis. J Biomed Res. 2014; 28:25–39. [PubMed: 24474961]
16. Sprague AH, Khalil RA. Inflammatory cytokines in vascular dysfunction and vascular disease. Biochem Pharmacol. 2009; 78:539–52. [PubMed: 19413999]
17. Zhu W-H, MacIntyre A, Nicosia RF. Regulation of angiogenesis by vascular endothelial growth factor and angiopoietin-1 in the rat aorta model: Distinct temporal patterns of intracellular signaling correlate with induction of angiogenic sprouting. Am J Pathol. 2002; 161:823–30. [PubMed: 12213710]
18. Zhang W, Liu HT. MAPK signal pathways in the regulation of cell proliferation in mammalian cells. Cell Res. 2002; 12:9–18. [PubMed: 11942415]
19. Kim EK, Choi E-J. Pathological roles of MAPK signaling pathways in human diseases. Biochim Biophys Acta. 2010; 1802:396–405. [PubMed: 20079433]
20. Huang X, Yang N, Fiore VF, Barker TH, Sun Y, Morris SW, et al. Matrix stiffness–induced myofibroblast differentiation is mediated by intrinsic mechanotransduction. Am J Respir Cell Mol Biol. 2012; 47:340–8. [PubMed: 22461426]
21. Scott NA, Cipolla GD, Ross CE, Dunn B, Martin FH, Simonet L, et al. Identification of a potential role for the adventitia in vascular lesion formation after balloon overstretch injury of porcine coronary arteries. Circulation. 1996; 93:2178–87. [PubMed: 8925587]
22. Sehgel NL, Vatner SF, Meininger GA. “Smooth Muscle Cell Stiffness Syndrome”-Revisiting the Structural Basis of Arterial Stiffness. Front Physiol. 2015; 6:335. [PubMed: 26635621]
23. Kohn JC, Lampi MC, Reinhart-King CA. Age-related vascular stiffening: causes and consequences. Front Genet. 2015; 6:112. [PubMed: 25926844]
24. Grant CA, Twigg PC. Pseudostatic and dynamic nanomechanics of the tunica adventitia in elastic arteries using atomic force microscopy. ACS Nano. 2013; 7:456–64. [PubMed: 23241059]
25. Arora PD, Narani N, McCulloch CAG. The compliance of collagen gels regulates transforming growth factor-β induction of α-smooth muscle actin in fibroblasts. Am J Pathol. 1999; 154:871–82. [PubMed: 10079265]
26. Goffin JM, Pittet P, Csucs G, Lussi JW, Meister J-J, Hinz B. Focal adhesion size controls tension-dependent recruitment of α-smooth muscle actin to stress fibers. J Cell Biol. 2006; 172:259–68. [PubMed: 16401722]
27. Shi Y, O’Brien JE, Fard A, Mannion JD, Wang D, Zalewski A. Adventitial myofibroblasts contribute to neointimal formation in injured porcine coronary arteries. Circulation. 1996; 94:1655–64. [PubMed: 8840858]

28. Zhang L, Li Y, Liu Y, Wang X, Chen M, Xing Y, et al. STAT3-mediated MMP-2 expression is required for 15-HETE-induced vascular adventitial fibroblast migration. J Steroid Biochem Mol Biol. 2015; 149:106–17. [PubMed: 25623089]
29. Kloxin AM, Benton JA, Anseth KS. In situ elasticity modulation with dynamic substrates to direct cell phenotype. Biomaterials. 2010; 31:1–8. [PubMed: 19788947]
30. Liu F, Mih JD, Shea BS, Kho AT, Sharif AS, Tager AM, et al. Feedback amplification of fibrosis through matrix stiffening and COX-2 suppression. J Cell Biol. 2010; 190:693–706. [PubMed: 20733059]
31. Mabry KM, Lawrence RL, Anseth KS. Dynamic stiffening of poly(ethylene glycol)-based hydrogels to direct valvular interstitial cell phenotype in a three-dimensional environment. Biomaterials. 2015; 49:47–56. [PubMed: 25725554]
32. Mahadevaiah S, Robinson KG, Kharkar PM, Kiick KL, Akins RE. Decreasing matrix modulus of PEG hydrogels induces a vascular phenotype in human cord blood stem cells. Biomaterials. 2015; 62:24–34. [PubMed: 26016692]
33. Bryant, S., Anseth, K. Scaffolding In Tissue Engineering. CRC Press; 2005. Photopolymerization of Hydrogel Scaffolds; p. 71-90.
34. Kharkar PM, Kiick KL, Kloxin AM. Design of thiol- and light-sensitive degradable hydrogels using Michael-type addition reactions. Polymer Chemistry. 2015; 6:5565–74. [PubMed: 26284125]
35. Liang Y, Coffin MV, Manceva SD, Chichester JA, Jones RM, Kiick KL. Controlled release of an anthrax toxin-neutralizing antibody from hydrolytically degradable polyethylene glycol hydrogels. J Biomed Mater Res A. 2016; 104:113–23. [PubMed: 26223817]
36. Kwon HM, Sangiorgi G, Ritman EL, Lerman A, McKenna C, Virmani R, et al. Adventitial vasa vasorum in balloon-injured coronary arteries: Visualization and quantitation by a microscopic three-dimensional computed tomography technique. J Am Coll Cardiol. 1998; 32:2072–9. [PubMed: 9857895]
37. Cai W-J, Koltai S, Kocsis E, Scholz D, Kostin S, Luo X, et al. Remodeling of the adventitia during coronary arteriogenesis. American Journal of Physiology - Heart and Circulatory Physiology. 2003; 284:H31–H40. [PubMed: 12388238]
38. Dong Y, Xie X, Wang Z, Hu C, Zheng Q, Wang Y, et al. Increasing matrix stiffness upregulates vascular endothelial growth factor expression in hepatocellular carcinoma cells mediated by integrin β1. Biochem Biophys Res Commun. 2014; 444:427–32. [PubMed: 24472554]
39. Church AC, Martin DH, Wadsworth R, Bryson G, Fisher AJ, Welsh DJ, et al. The reversal of pulmonary vascular remodeling through inhibition of p38 MAPK-alpha: a potential novel anti-inflammatory strategy in pulmonary hypertension. Am J Physiol Lung Cell Mol Physiol. 2015; 309:L333–L47. [PubMed: 26024891]
40. Wu J, Thabet SR, Kirabo A, Trott DW, Saleh MA, Xiao L, et al. Inflammation and Mechanical Stretch Promote Aortic Stiffening in Hypertension Through Activation of p38 MAP Kinase. Circulation research. 2014; 114:616–25. [PubMed: 24347665]
41. Li G, Chen S-J, Oparil S, Chen Y-F, Thompson JA. Direct in vivo evidence demonstrating neointimal migration of adventitial fibroblasts after balloon injury of rat carotid arteries. Circulation. 2000; 101:1362–5. [PubMed: 10736277]
42. Driesen RB, Nagaraju CK, Abi-Char J, Coenen T, Lijnen PJ, Fagard RH, et al. Reversible and irreversible differentiation of cardiac fibroblasts. Cardiovasc Res. 2014; 101:411–22. [PubMed: 24368833]
43. Wang H, Tibbitt MW, Langer SJ, Leinwand LA, Anseth KS. Hydrogels preserve native phenotypes of valvular fibroblasts through an elasticity-regulated PI3K/AKT pathway. Proc Natl Acad Sci U S A. 2013; 110:19336–41. [PubMed: 24218588]
44. Liu F, Mih JD, Shea BS, Kho AT, Sharif AS, Tager AM, et al. Feedback amplification of fibrosis through matrix stiffening and COX-2 suppression. The Journal of Cell Biology. 2010; 190:693–706. [PubMed: 20733059]
45. Peyton SR, Putnam AJ. Extracellular matrix rigidity governs smooth muscle cell motility in a biphasic fashion. Journal of Cellular Physiology. 2005; 204:198–209. [PubMed: 15669099]

46. Katelyn ES-R, Jason BP, Hannah PK, Allison T, Joshua AH, Amy BH, et al. The impact of laminin on 3D neurite extension in collagen gels. Journal of Neural Engineering. 2012; 9:046007. [PubMed: 22736189]

47. Jabbari E, Sarvestani SK, Daneshian L, Moeinzadeh S. Optimum 3D Matrix Stiffness for Maintenance of Cancer Stem Cells Is Dependent on Tissue Origin of Cancer Cells. PLOS ONE. 2015; 10:e0132377. [PubMed: 26168187]

48. Chae CU, Lee RT, Rifai N, Ridker PM. Blood pressure and inflammation in apparently healthy men. Hypertension. 2001; 38:399–403. [PubMed: 11566912]

49. Gao Q, Guo M, Zeng W, Wang Y, Yang L, Pang X, et al. Matrix metalloproteinase 9 secreted by hypoxia cardiac fibroblasts triggers cardiac stem cell migration in vitro. Stem Cells International. 2015; 2015:12.

50. Burke DL, Frid MG, Kunrath CL, Karoor V, Anwar A, Wagner BD, et al. Sustained hypoxia promotes the development of a pulmonary artery-specific chronic inflammatory microenvironment. Am J Physiol Lung Cell Mol Physiol. 2009; 297:L238–L50. [PubMed: 19465514]

51. Valabhji J, Dhanjil S, Nicolaides AN, Elkeles RS, Sharp P. Correlation between carotid artery distensibility and serum vascular endothelial growth factor concentrations in type 1 diabetic subjects and nondiabetic subjects. Metabolism. 2001; 50:825–9. [PubMed: 11436189]

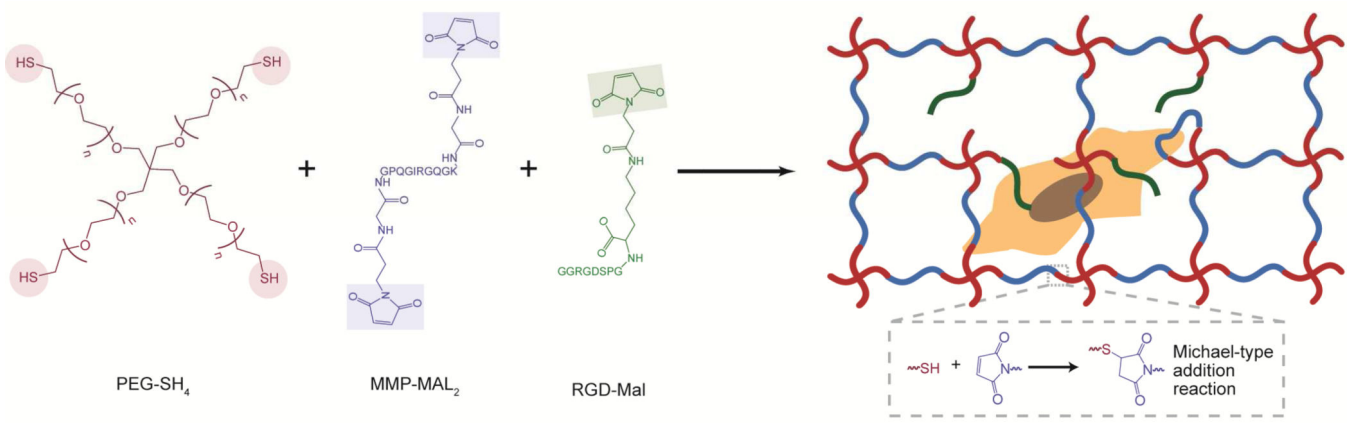

Fig. 1. Enzymatically degradable hydrogel formation

Hydrogels were formed by reacting thiol end-functionalized, four-arm PEG macromers ($PEG\text{-}SH_4$) with bis-maleimide, end-functionalized, cell degradable crosslinker peptides ($MMP\text{-}Mal_2$) and monomaleimide pendent RGD peptides (RGD-Mal) using a Michael-type addition reaction.

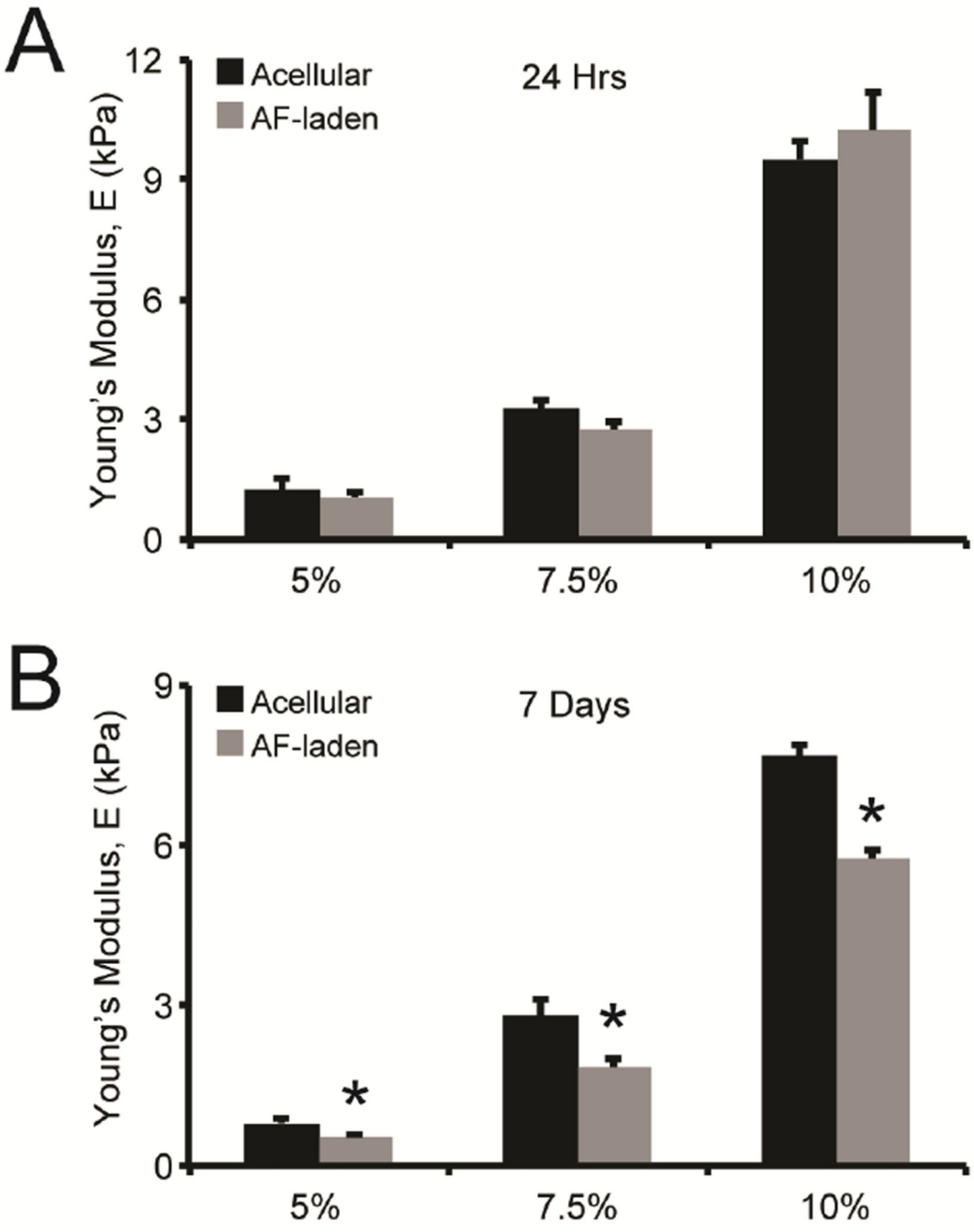

Fig. 2. Rheological characterization and AF-mediated remodeling of hydrogels

Hydrogels were formed and cultured in cell culture medium prior to characterization via oscillatory shear rheology at defined time points. (A) 5%, 7.5%, and 10% hydrogels exhibited significantly different swollen Young's moduli after 24 hrs. AF encapsulation did not alter gel modulus after 24 hrs of culture, compared to control hydrogels. (B) After 7 days of culture, the Young's modulus of AF-laden hydrogels was significantly decreased compared to paired controls for all weight percent hydrogels. * indicates significance from control hydrogels ($p<0.05$ by ANOVA with Tukey HSD). N=3.

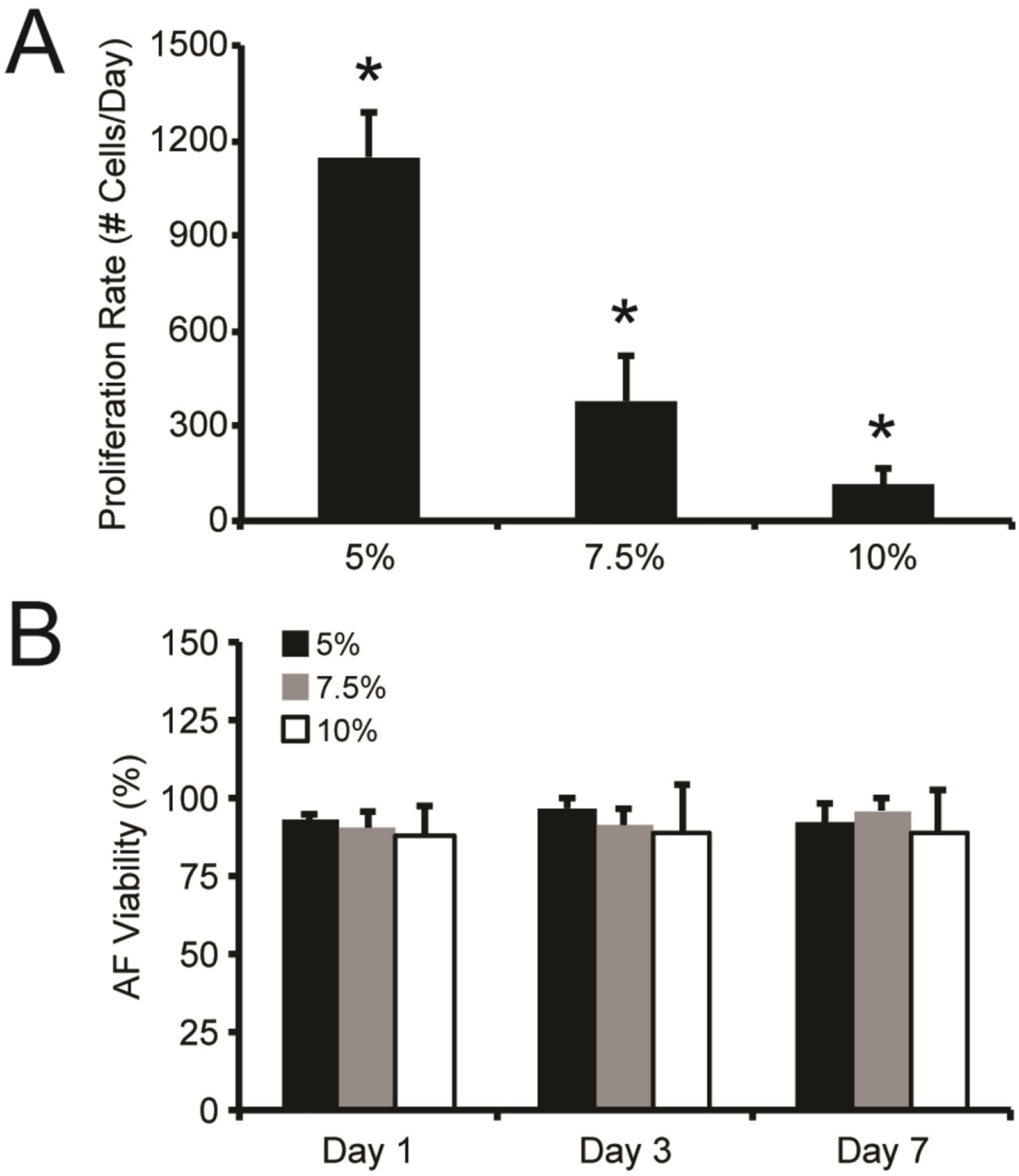

Fig. 3. AF proliferation and viability in PEG hydrogels

(A) The proliferation rate of AFs encapsulated in 5%, 7.5%, and 10% hydrogels significantly decreased with increasing weight percent. (B) Over 90% viability was observed for AFs encapsulated 5%, 7.5%, and 10% PEG gels over the course of 7 days. * represents significance from other w/v% gels ($p<0.05$ by ANOVA with Tukey HSD). N=3.

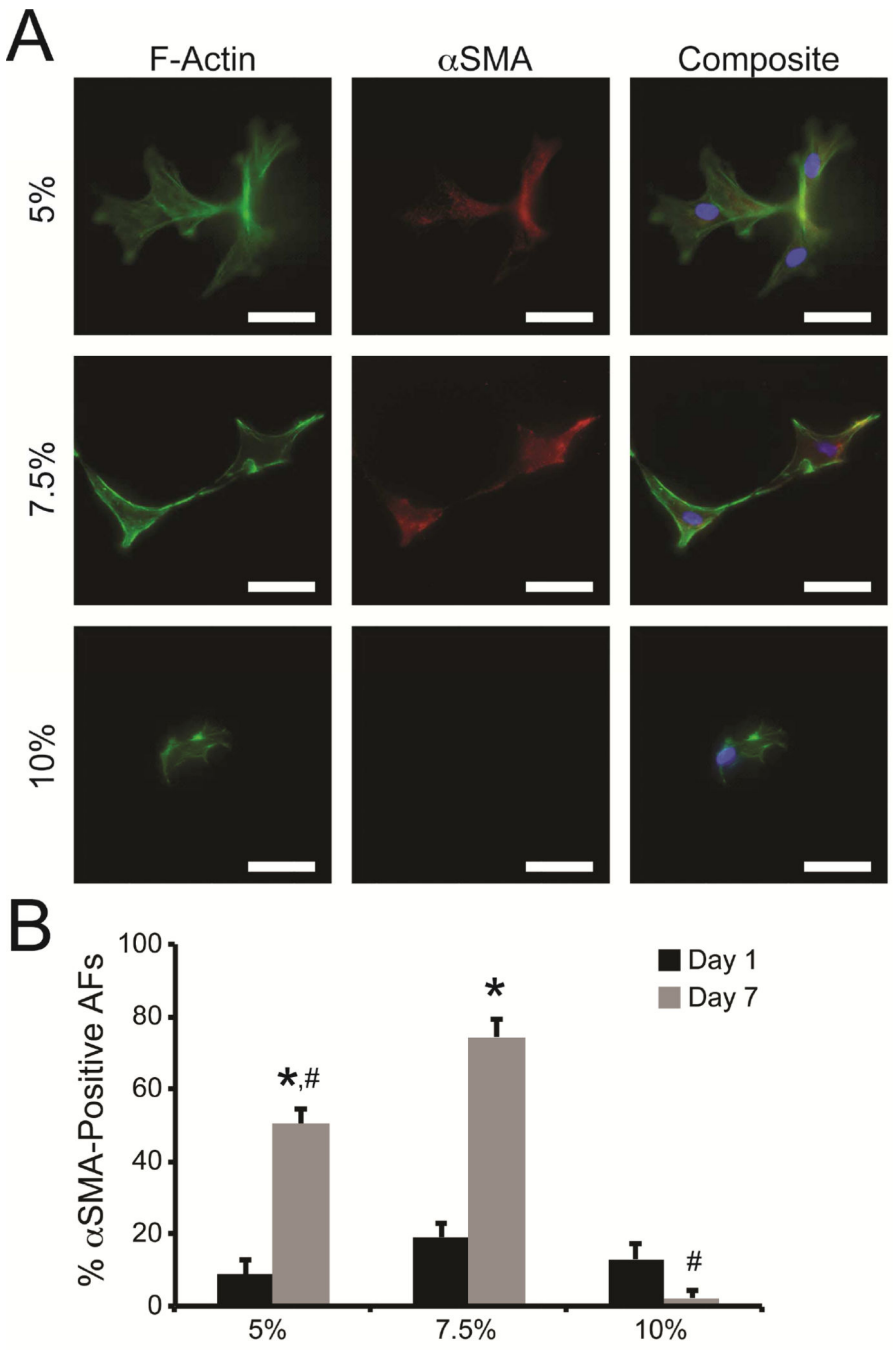

Fig. 4. Myofibroblast activation in response to hydrogel stiffness

(A) Representative images of AFs cultured in 5%, 7.5%, and 10% hydrogels for 7 days. AFs were stained with antibodies for F-actin (green), αSMA (red), and nuclear stain Hoescht 33342 (blue). Scale bars = 50 μm. (B) Low levels of αSMA-positive AFs were detected in all hydrogels after 1 day of culture. After 7 days of culture, an increased number of AFs elicited αSMA staining in 5% and 7.5% hydrogels, while very few αSMA-positive cells were observed in 10% hydrogels. * represents significance from paired hydrogels on day 1;

represents significance from 7.5% hydrogels on day 7 ($p<0.05$ by two-way ANOVA with Tukey HSD).

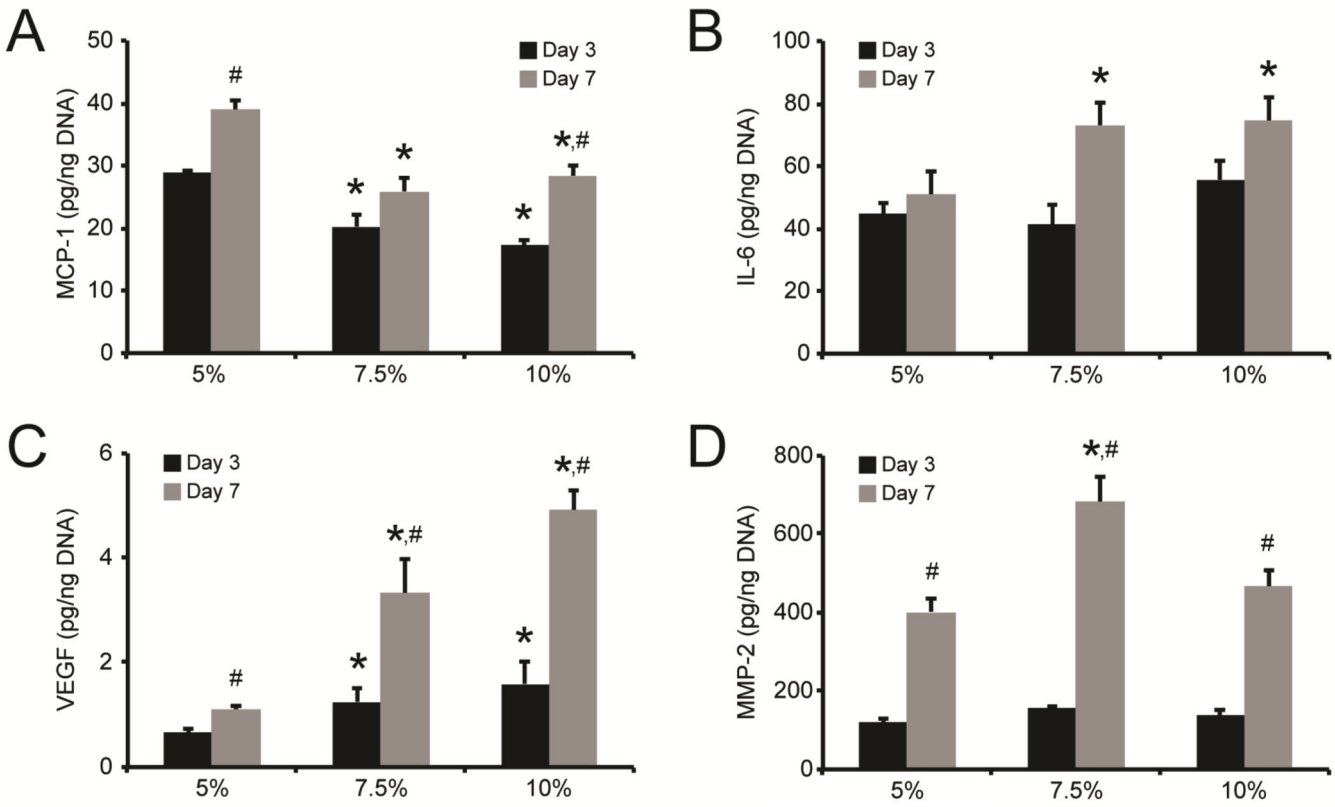

Fig. 5. AF secretion of inflammatory, angiogenic, and matrix remodeling factors in response to hydrogel modulus

AF secretion of (A) MCP-1, (B) IL-6, (C) VEGF, and (D) MMP-2 following culture in 5%, 7.5%, and 10% hydrogels for either 3 or 7 days. * represents significance from 5% hydrogels; # represents significance from paired hydrogels on day 3 ($p<0.05$ by two ANOVA with Tukey HSD). N=3.

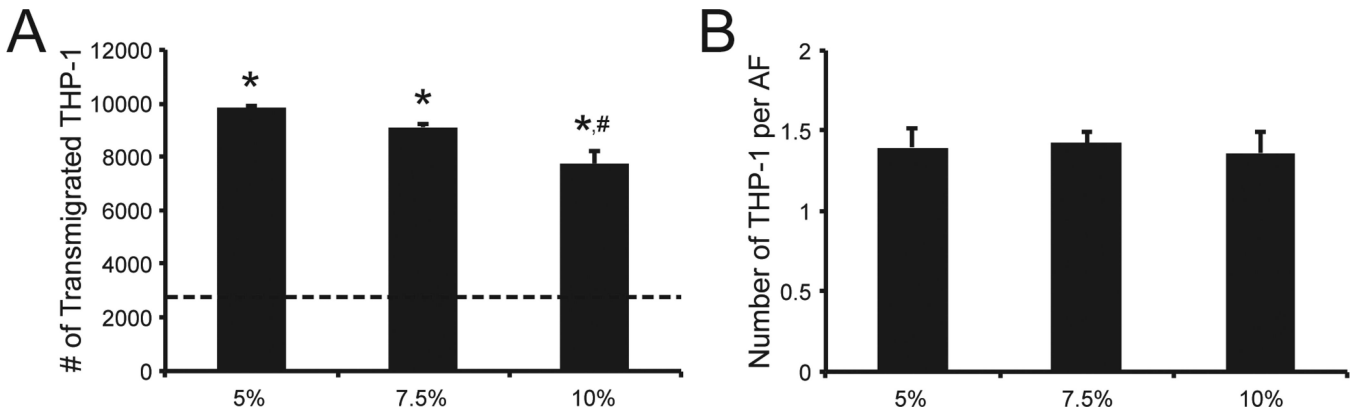

Fig. 6. THP-1 monocyte recruitment is modulus dependent

Conditioned medium (CM) was collected from AF-laden and acellular hydrogels after 3 days of culture; THP-1 monocyte transmigration in response to CM was then measured after 2 hrs, using a Boyden chamber migration assay. (A) Overall, significantly more THP-1 monocytes transmigrated in response to CM collected from AF-laden hydrogels, compared to SCGM alone (dotted line). Interestingly, THP-1 transmigration was significantly decreased in CM obtained from AF-laden 10% gels, compared to CM from softer AF-laden 5% gels. (B) However, when the number of transmigrated THP-1 cells was normalized to the number of AFs in each corresponding gel, no differences were observed across hydrogel formulations. * represents significance from fresh SCGM medium and acellular hydrogel controls; # represents significance from AF-laden 5% hydrogels ($p<0.05$ by ANOVA with Tukey HSD). N=3.

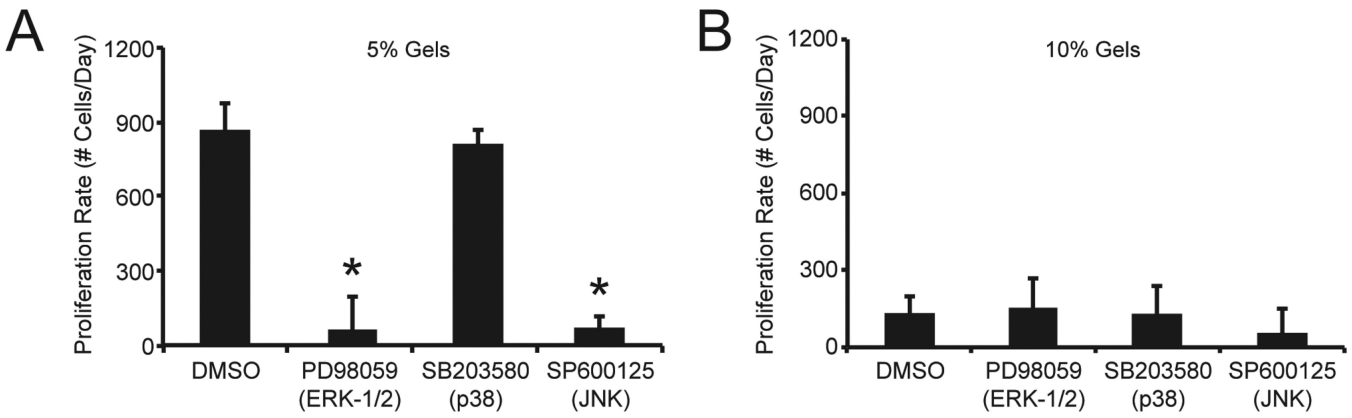

Fig. 7. AF proliferation rate in 5% and 10% hydrogels with MAPK inhibitors

Following encapsulation in (A) 5% and (B) 10% hydrogels, AFs were treated with ERK-1/2 pathway inhibitor PD98059 (10 μmol/L), the p38 inhibitor SB203580 (10 μmol/L), or the JNK inhibitor SP600125 (10 μmol/L). (A) In 5% hydrogels, AF proliferation rate was significantly decreased when gels were treated with JNK inhibitor SP600125 or the ERK pathway inhibitor PD98059. However, AF proliferation rate in 5% gels was not altered when treated with the p38 inhibitor SB203580. (B) In 10% hydrogels, proliferation rate was not altered when ERK-1/2, p38, or JNK pathways were inhibited. * represents significance from DMSO-treated control gels ($p<0.05$ by ANOVA with Tukey HSD). N=3.

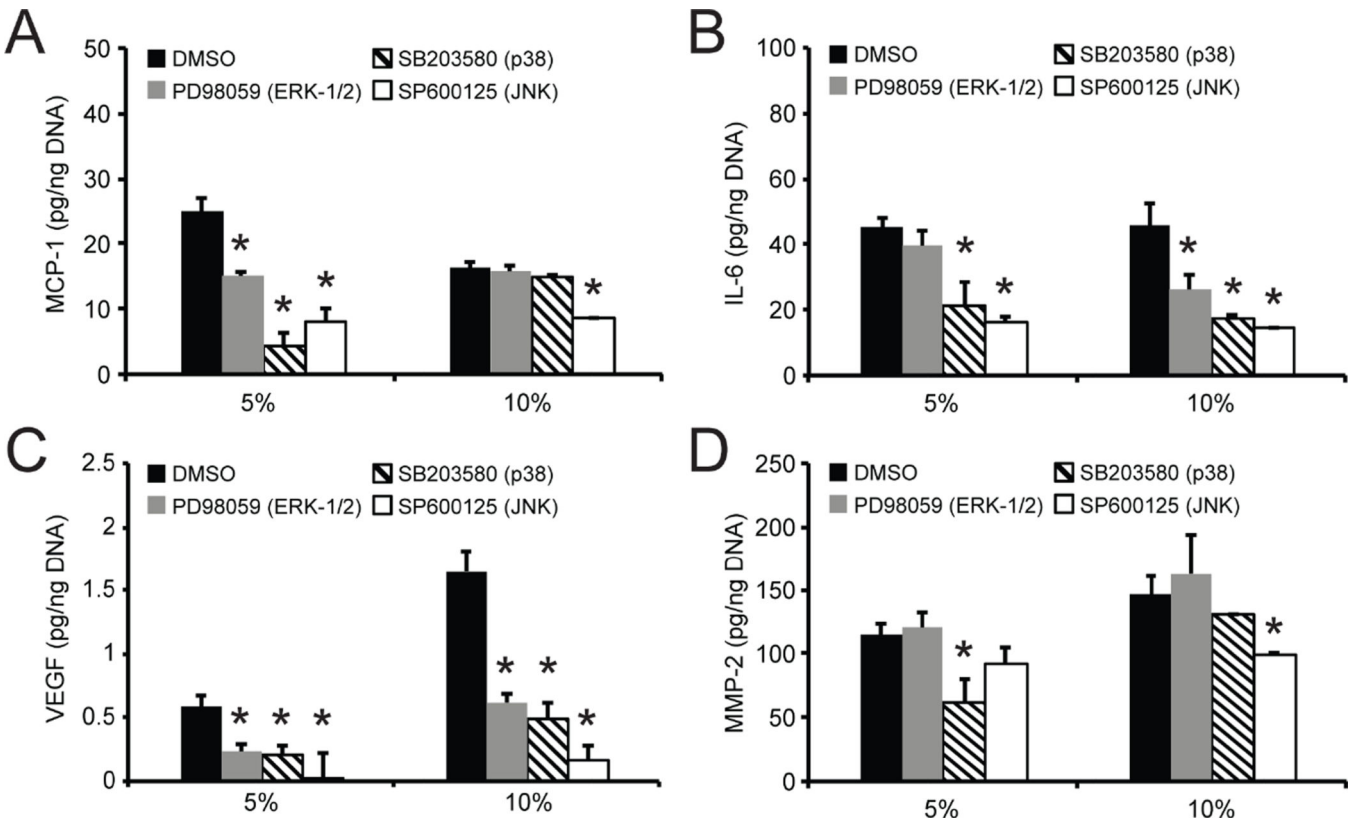

Fig. 8. Protein secretion is differentially regulated by MAPK signaling pathway in 5% versus 10% hydrogels

Following encapsulation in 5% and 10% hydrogels, AFs were treated with ERK-1/2 pathway inhibitor PD98059 (10 μmol/L), the p38 inhibitor SB203580 (10 μmol/L), or the JNK inhibitor SP600125 (10 μmol/L). After 3 days of culture, production of (A) MCP-1, (B) IL-6, (C) VEGF, and (D) MMP-2 by AFs encapsulated in 5% and 10% hydrogels was examined. * represents significance from DMSO-treated control gels ($p<0.05$ by ANOVA with Tukey HSD). N=3.

Table 1

Summary of the impact of ERK-1/2, p38, and JNK pathway inhibition on AF proliferation and cytokine production.

MAPK Subfamily	Proliferation Rate	MCP-1	IL-6	VEGF	MMP-2
5% Hydrogel					
ERK Inhibition	↓	↓	-	↓↓	-
p38 Inhibition	-	↓↓↓	↓↓	↓↓	↓
JNK Inhibition	↓↓	↓↓↓	↓↓	↓↓↓	-
10% Hydrogel					
ERK Inhibition	-	-	↓↓	↓↓	-
p38 Inhibition	-	-	↓↓	↓↓↓	-
JNK Inhibition	-	↓↓	↓↓↓	↓↓↓	↓

Arrows represent decreased AF proliferation rate or production of signaling factors due to inhibition of specific MAPK subfamily member.

↓ 25–50% reduction;

↓↓ 51–75% reduction;

↓↓↓ 76–100% reduction.

No significant changes following inhibition of MAPK subfamily member are indicated by ‘-‘.